

GAIN AND LOSS MECHANISMS IN InGaAs/InGaAsP MULTI-QUANTUM-WELL LASER STRUCTURES

A. Hoffmann, M. Tischel, R. Heitz, L. Podlowski
Technische Universität Berlin, Hardenbergstr. 36, D-1000 Berlin 12

M. Rosenzweig*, M. Möhrle
Heinrich-Hertz-Institut, Einsteinufer 37, D-1000 Berlin 10
*present address: Technische Fachhochschule Berlin, Oudenarder Str. 64,
D-1000 Berlin 65

(Received 4 August 1992)

InGaAs/InGaAsP-multi-quantum-well-separate-confinement-heterostructure (MQW-SCH) layers are favoured as the active region in long-wavelength semiconductor lasers. In order to discuss the gain and loss mechanisms in these layers gain and luminescence spectra for different excitation densities and temperatures down to $T=1.8\text{K}$, and calorimetric absorption spectra have been measured and analyzed for 8nm thick InGaAs-wells and 10nm thick InGaAsP-barriers. The injection efficiency is about 75% and independent of carrier density. There are internal optical losses which increase with increasing carrier density. Calorimetric absorption spectra indicate the existence of further electronic states with nonradiative transitions. We assume that these are interface states between wells and barriers.

1. Introduction:

Optical communication and signal processing systems require low threshold current semiconductor lasers with an emission wavelength at the attenuation minimum of optical fibres ($1.55\mu\text{m}$). Of special interest are InGaAs/InGaAsP multi-quantum-well (MQW)-lasers [1,2,3] due to their theoretically expected advantages over conventional InGaAsP-double heterostructure (DH)-lasers, such as lower threshold currents, improved temperature behaviour, frequency response, spectral line width and chirping [1]. Experimental results of such lasers indicate much less improved laser properties, especially threshold currents, than observed with short wavelength GaAs/GaAlAs-MQW-lasers.

The purpose of this work is to investigate InGaAs/InGaAsP-MQW-separate confinement heterostructures (SCH) concerning the electrical and optical excited gain at room temperature and the optical properties as gain, luminescence, transmission, and calorimetric absorption spectroscopy at low temperatures in order to identify the electronic transitions responsible for gain and loss in semiconductor lasers.

2. Experiments:

The laser structures were grown by low pressure metal-organic-vapour-phase epitaxy (MOVPE) on n-InP-substrates. The active layer consists of InGaAs wells of a thickness d of about 8nm, corresponding to an emission wavelength of $1.55\mu\text{m}$, and InGaAsP ($\lambda_g=1.3\mu\text{m}$)-barrier layers of 10nm width. The MQW-structure is sandwiched between InGaAsP-material of the same composition as the barriers to form a transverse optical waveguide with a total thickness of 300nm. The wells, the barriers, and the upper part of the waveguide are not doped intentionally, whereas the lower part of the waveguide is n-doped. The waveguide layer is followed by a p-doped InP-confinement layer and a heavily p-doped InGaAs contact layer. For optically excited measurements this contact layer is removed by selective wet chemical etching. Structures with 2, 4 and 8 wells were examined.

For use as semiconductor lasers in communication or signal processing systems the dependence of optical gain on injected carrier density is the most essential feature. In an electrical excited laser at threshold the effective gain G compensates the losses

due to absorption α and emitted light. The maximum of gain therefore is

$$g_{\max} = G/N_z \Gamma = \frac{1}{N_z \Gamma} \left(\alpha - \frac{\ln(R_1 R_2)}{2L} \right) \quad (1)$$

N_z is the number of wells, L is the length of the cavity, Γ the confinement factor of one well, and $R_1 R_2$ are the reflectivities of the mirrors. The corresponding carrier density N_{elec} can be deduced from the threshold current I_{th} , the injection efficiency η_{inj} , the excited volume V and the carrier lifetime τ .

$$N(\text{elec}) = I_{\text{th}} \tau e_0^{-1} V^{-1} = I_{\text{th}} \eta_{\text{inj}} \tau (b \cdot L \cdot d \cdot e_0 \cdot N_z)^{-1} \quad (2)$$

d is the thickness of one well, e_0 is elementary charge, and b is the width of the active layer.

In fig. 1 the dependence of the maximum of gain on carrier density is plotted. The confinement factor Γ is calculated using the mode matching method, the reflectivities are determined with aid of Fresnel's formula and the effective refractive index, the absorption coefficient α is deduced from the external quantum efficiency and τ from turn on delay measurements of electrically excited lasers. The injection efficiency was taken to be $\eta_{\text{inj}} = 1$. The data are normalized to one well to prove the homogeneity at carrier injection. The plot results in one straight line using a logarithmic scale for the carrier density as expected from theory /4,5/, which verifies the relatively large threshold currents of lasers of medium and short cavity lengths.

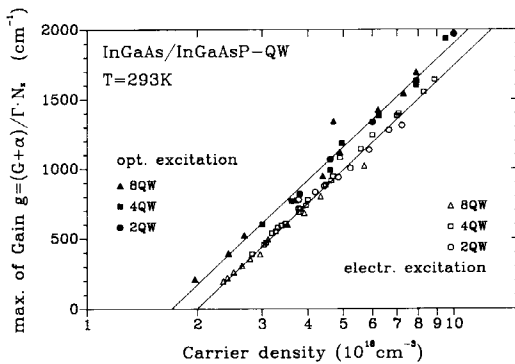


Fig. 1: The dependence of the density gain on injected carrier density.

In order to determine the exact value of the injection efficiency η_{inj} optically excited gain spectra have been measured. In this case the carriers of inverse electrical charge are created at the same spatial position, any injection losses can be neglected. The optically excited carrier density N_{opt} is proportional to the excitation density D_{exc} , the absorption coefficient

α_{exc} of the wells for the excitation wavelength λ_{exc} , the carrier lifetime τ , and the thickness of the active layer d .

$$N_{\text{opt}} = D_{\text{exc}} (1 - e^{-N_z d \alpha_{\text{exc}}}) \frac{\tau \lambda_{\text{exc}}}{h c_0 N_z d} \quad (3)$$

h is the Planck's constant, and c_0 is the vacuum light velocity.

For excitation we used a Q switched Nd:YAG laser with an excitation pulse length of 250ns ($\lambda = 1.06\mu\text{m}$). The effective gain G is deduced from the ratio of amplified spontaneous emission for excitation with stripes of different lengths /5/. The maximum of gain of a single well is calculated ($g_m = (G_m + \alpha) / N_z \Gamma$) and plotted in fig.1 as a straight line. The logarithmic dependence of optical gain on carrier density is confirmed, but the optical excitation curve is shifted to smaller carrier densities, whereas the slope is the same.

Optical gain spectroscopy has been employed at low temperatures down to $T = 17\text{K}$. In fig.2 gain spectra for different temperatures but constant excitation density are plotted for a sample with 8 wells. The spectra (290K) show two gain maxima, one at $1.55\mu\text{m}$ and the second at $1.33\mu\text{m}$. The gain maximum at $1.33\mu\text{m}$ is attributed to the waveguide, which is excited by the pumping Nd:YAG laser, too; the spectral behaviour of the waveguide gain is not

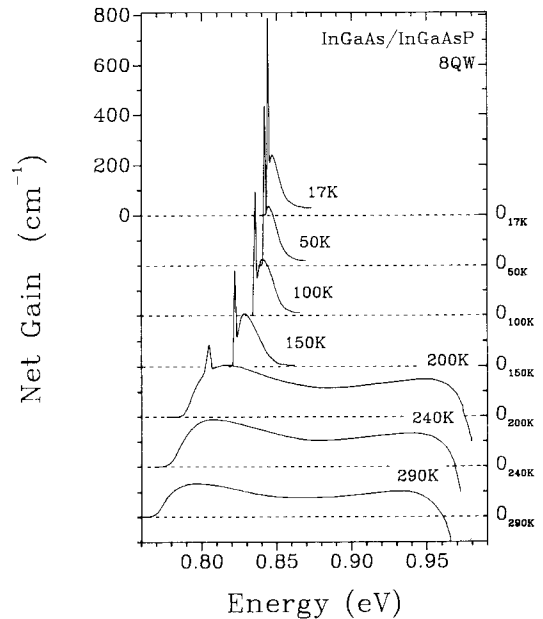


Fig. 2: Gain spectra at different temperatures of a wafer with 8 quantum wells for an excitation density of $P = 200\text{kWcm}^{-2}$.

discussed in this paper (but is in /5/), and therefore neglected in the spectra at lower temperatures. With decreasing temperatures the spectral width of the gain around 1.5 μ m decreases, while the gain values rise absolutely. At about T=200K on the low energy side of the spectra a sharp spike appears and becomes the dominant structure in the spectra with further decreasing temperature. Samples with 2 and 4 wells show a similar behaviour. The appearance of the spike depends on temperature and excitation density. With decreasing temperature the excitation density, necessary to create the spike, decreases, too.

In fig.3 the gain spectrum is compared to the transmission spectrum and the photoluminescence spectrum measured at low temperatures. The luminescence band (E_1) is slightly shifted to lower energies compared to the transmission minimum. An explanation for this Stokes shift which is typical in MQW semiconductors is given in /6/. Two additional luminescence maxima exist at much lower energies (E_2 and E_3). The broad band gain maximum coincides with the luminescence band, whereas the small spike is spectrally located at the long wavelength end of the luminescence band E_1 . The dependence of the photoluminescence on (relatively low) excitation density is plotted in fig.4. With increasing excitation density a luminescence band E_2' appears on the high energy side of E_2 . Its intensity increases superlinearly with excitation densities and the maximum is shifted to higher energies.

Finally, calorimetric absorption spectra were taken at temperatures of T=45mK (see fig. 5). In the transmission spectrum (upper curve) the $n=1$

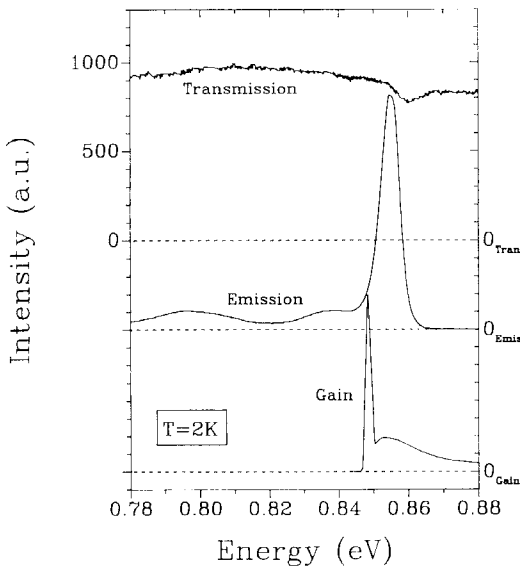


Fig. 3: Luminescence, transmission and gain spectra of a wafer with 8 quantum wells at T=2K.

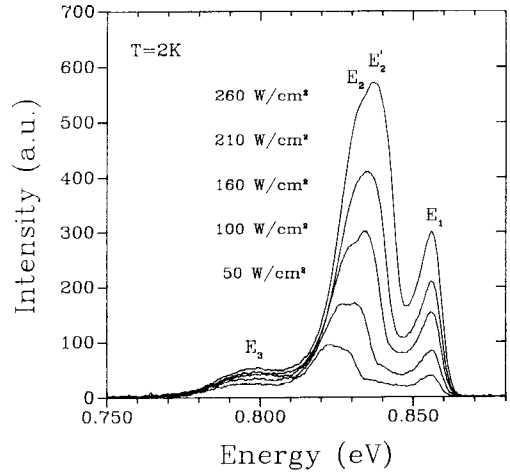


Fig. 4: Luminescence spectra of a wafer with 2 quantum wells for different excitation densities.

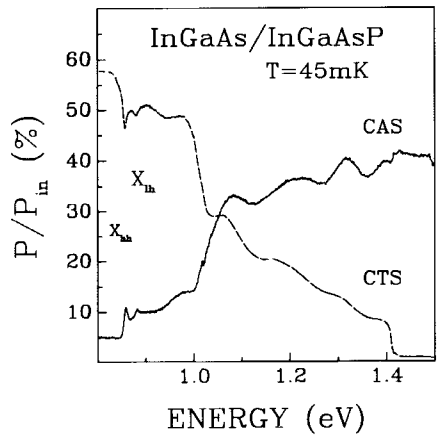


Fig. 5: Calorimetric absorption (CAS) and transmission (CTS) spectra of a wafer with 8 quantum wells.

quantum-well-transition of the heavy and light holes can be clearly observed. In the corresponding calorimetric absorption spectrum (lower curve) maxima of warming up are to be seen which coincide with the transmission minima. The deduced quantum efficiency for radiative transitions is about $\eta_{rad} = 52\%$.

3. Discussion:

The observed logarithmic dependence of gain on carrier density verifies theoretical calculations /4,5/

of optical gain in InGaAs/InGaAsP-MQW-structures. For carrier lifetimes not strongly varying with carrier density it can be transformed in a logarithmic dependence of gain on current density:

$$g = \beta J_0 \ln (\eta_{inj} J / J_0 N_T)$$

J is the injection current density, J_0 is the transparency current density, and β is the differential gain at the transparency current density.

The fact that the gain-carrier-density relation is independent of the number of wells of the examined sample reveals a homogeneous electrical injection up to 8 wells. The parallel shift of the curves for electrical and optical excitation can be interpreted as a carrier density independent electrical injection efficiency of about $\eta_{inj} = 75\%$ which is in agreement with the observed internal quantum efficiency of lasers with large cavity lengths. Furthermore, the parallel shift indicates that the observed carrier dependent losses are independent of the excitation mechanism. Since these losses increase with increasing carrier density they can be attributed to intervalence-band-absorption between the heavy-hole valence-band and the spin-orbit-split-off valence band and free carrier absorption.

The general behaviour of optical gain in dependence on temperature is in agreement with the corresponding shift of bandgap and fermi energies. Much more interesting is the appearance of the spike at specific temperatures depending on the excitation density. Similar effects have been observed in spectra of comparably thick InGaAsP layers with a bandgap corresponding to an emission wavelength of $1.55\mu\text{m}$. This excludes the quantum confined exciton from being responsible for the peak. The spectral shift between transmission and photoluminescence spectra indicates that the radiative recombinations at low temperatures and low excitation densities prefer transitions between electronic states with energy differences slightly smaller than the band gap. The electronic states might be free and bound excitons on shallow donors and acceptors. The small binding energy is quite in accordance with the small effective masses. The spike in the gain spectrum itself is located at the long wavelength bottom of the luminescence spectra. As there exists no corresponding luminescence line for low density excitation a specific impurity transition can be neglected, too. On the other hand, in fig.4 a new emission line labeled E_2' is observed between the fundamental emission band E_1 and the emission E_2 which shifts to smaller wavelengths with increasing excitation density. We assume that the electronic transition which creates this luminescence is responsible for the gain peak, too. From its behaviour it is attributed to the radiative recombination of an electron-hole plasma, which can occur in thin layers at much lower excitation densities than in commonly used "three dimensional" ma-

terials. This behaviour is in agreement with investigations in /7/.

Finally, the calorimetric absorption spectra have to be discussed. Any further transition than the well-gap and shallow impurities can be observed. Most interesting is the relatively small quantum efficiency for radiative transitions of 52%. This cannot be explained by the observed small spectral shift between absorption and luminescence. In our opinion the heating is due to nonradiative transition via interface states between the InGaAs-wells and the InGaAsP-barriers, which might result from the gas-composition switching procedure during the growth of such layers.

4. Conclusion

The careful analysis of optical properties of InGaAs/InGaAsP-MQW-SCH laser structures results in the following: The electrical excitation is homogeneous for layers up to 8 wells. The electrical injection efficiency is about 75% and independent of carrier density. There are internal optical losses increasing with carrier density which might originate from intervalence band absorption and free carrier absorption. At room temperature all shallow impurities are ionized and stimulated emission is due to transitions of free carriers. At low temperature the impurities participate to the stimulated emission, too. At high excitation densities an electron-hole-plasma is created. Although the wells and barriers are not intentionally doped the calorimetric measurements indicate the existence of further interface states with nonradiative transitions. We assume that they are surface states of the boundaries between wells and barriers.

References:

- /1/ U. Koren, B.I. Hiller, Y.K. Su, T.L. Koch, and J.E. Bowers, *Appl.Phys.Lett.* **51**, 1744 (1987)
- /2/ M. Kitamura, S. Takano, T. Sasaki, H. Yamada, and I. Mito, *Appl.Phys.Lett.* **53**, 1 (1988)
- /3/ R.W. Glew, B. Garrett, and P.D. Greene, *Electron. Lett.* **25**, 1103 (1989)
- /4/ M. Rosenzweig, M. Mohrle, H. Düser, and H. Venghaus, *IEEE J. of Quantum Electr.*, Vol **27**, 1804 (1991)
- /5/ M. Rosenzweig, M. Mohrle, H. Düser, M. Tischel, R. Heitz, and A. Hoffmann, *SPIE Vol.* **1362**, 876 (1990)
- /6/ F. Yang, B. Henderson, and K.P. O'Donnell, 7th Trieste symposium on wide-band-gap semiconductors, 1992, to be published in *physica b*
- /7/ M. Gal, J.M. Viner, P.C. Taylor, C.P. Kuo, R.M. Cohen, and G.B. Stringfellow, *J. Appl. Phys.* **58**(2), 948 (1985)